REVIEW

Analytical ultracentrifuge: an ideal tool for characterization of non-coding RNAs

Maulik D. Badmalia[1] · M. Quadir Siddiqui[1] · Tyler Mrozowich[1] · Darren L. Gemmill[1] · Trushar R. Patel[1,2,3]

Abstract

Analytical ultracentrifugation (AUC) has emerged as a robust and reliable technique for biomolecular characterization with extraordinary sensitivity. AUC is widely used to study purity, conformational changes, biomolecular interactions, and stoichiometry. Furthermore, AUC is used to determine the molecular weight of biomolecules such as proteins, carbohydrates, and DNA and RNA. Due to the multifaceted role(s) of non-coding RNAs from viruses, prokaryotes, and eukaryotes, research aimed at understanding the structure–function relationships of non-coding RNAs is rapidly increasing. However, due to their large size, flexibility, complicated secondary structures, and conformations, structural studies of non-coding RNAs are challenging. In this review, we are summarizing the application of AUC to evaluate the homogeneity, interactions, and conformational changes of non-coding RNAs from adenovirus as well as from Murray Valley, Powassan, and West Nile viruses. We also discuss the application of AUC to characterize eukaryotic long non-coding RNAs, Xist, and HOTAIR. These examples highlight the significant role AUC can play in facilitating the structural determination of non-coding RNAs and their complexes.

Introduction to analytical ultracentrifuge

The development of the analytical ultracentrifuge (AUC) by Svedberg and colleagues in the 1920s revolutionized the characterization of biomolecules in solution (Svedberg and Pedersen 1940). In an AUC experiment, the preparation of biomolecules is subjected to high centrifugal force to accelerate their sedimentation governed by hydrodynamic principles, size and shape (Lebowitz et al. 2002; Mitra and Demeler 2020; Patel et al. 2016). The sedimentation of biomolecules is typically monitored by either exploiting the optical absorption of biomolecules at characteristic wavelengths or by Rayleigh interference (refractometric) optical systems (Crepeau et al. 1972; Harding and Rowe 1988). More recently, advances with fluorescence and multi-wavelength detection have proven to be another valuable alternative (Crepeau et al. 1972; Harding and Rowe 1988; Johnson et al. 2018; MacGregor et al. 2004; Wawra et al. 2019). AUC has emerged as an indispensable technique to investigate the shape, size, homogeneity, oligomeric state, and aggregation of biomolecules and macromolecular complexes, in solution with a minuscule amount of sample (~ 150–400 μL) (Liu et al. 2015; May et al. 2014; Schuck 2013; Wolff et al. 2015; Zhang et al. 2017a). There are numerous examples where AUC was used to study the conformations (initial, intermediate, and final) and ligand-induced changes of a biomolecule of interest (Brautigam et al. 2009; Dean et al. 2019; Matte et al. 2012; Mitra and Demeler 2020; Unzai

2018). AUC has also been used to study RNAs, and this review sheds light on employing AUC for biophysical characterization of RNA and RNA structure.

AUC experiments are categorized into two modes: sedimentation velocity (SV) and sedimentation equilibrium (SE). SV studies the evolution of the sedimentation process, whereas SE examines the final equilibrium distribution. Both SV and SE are complementary methods; both together provide an extensive characterization of mass, size, density, hydrodynamic shape, size distribution, purity, weak and reversible interactions, and the formation of multi-component complexes (Harding and Winzor 2001; Zhao et al. 2013). Under the SV mode, samples are spun at high angular velocity resulting in faster sedimentation of biomolecules. Using the bulk solute boundary, one can estimate the rate of sedimentation, which can be further exploited to calculate size, shape, and conformational homogeneity of the biomolecules under investigation.

On the other hand, during the SE experiment, the particles are spun at a slower speed compared to SV, to achieve a balance between the outward flux (flow due to sedimentation) and inward flux (flow due to diffusion). During the SE experiment, biomolecules are subjected to high diffusion forces, which result in increased buoyancy of the particles. This phenomenon helps us distinguish the molecules based on their stoichiometry and average molecular weight (Harding 1994; Rowe 2013). AUC data are collected by monitoring solute migration in case of SV-AUC, whereas in case of SE-AUC solute distribution is monitored; these data are then analyzed with mathematical relations that help us determine the stoichiometry, molecular weight, as well as other biophysical parameters. These mathematical steps have been explained at length elsewhere (Cole et al. 2008; Dam and Schuck 2004; Harding and Winzor 2001; Mitra 2009; Mitra and Demeler 2020; Patel et al. 2016).

Sophisticated programs have been developed which can reliably determine the sedimentation coefficient (s), as well as other hydrodynamic parameters for a biomolecular system of interest. Some of the routinely employed software packages include UltraScan-III (Brookes et al. 2010; Demeler and Gorbet 2016), SEDANAL (Sherwood and Stafford 2016), SEDFIT (Dam and Schuck 2004; Schuck 1998), and SVEDBERG (Philo 1997). There are many excellent reviews available on AUC methods, instrumentation, and data analysis, and readers should refer them for additional information (Arakawa and Philo 1999; Brautigam 2011; Cole and Hansen 1999; Cole et al. 2008; Fujita 1975; Gillis et al. 2014; Gorbet et al. 2018; Harding 1994; Harding et al. 2015; Harding and Winzor 2001; Laue and Stafford III 1999; Lebowitz et al. 2002; Liu et al. 2015; Patel et al. 2017b; Patel et al. 2016; Perkins et al. 2011; Planken and Colfen 2010; Schuck 2013; Schuster and Toedt 1996; Uchiyama et al. 2018; Unzai 2018; Yang et al. 2015). In this review,

we will focus on the application of AUC in studying non-coding RNAs.

Non-coding RNA: structures and challenges

Ribonucleic acid (RNA) is a biopolymer that forms an intermediary in gene expression and is responsible for the translation of genetic material—DNA to functional proteins. RNA is also one of the most important biopolymers performing various critical cellular roles including protein synthesis, gene regulation, and nucleic acid processing; the latter two processes are carried out by a class of RNA called non-coding RNAs (ncRNAs) (Kung et al. 2013; Novikova et al. 2013). ncRNA includes ribosomal RNA, transfer RNA, small ncRNA (< 200 nucleotides), and long ncRNA (lncRNA, > 200 nucleotides) (Mattick and Makunin 2006). LncRNAs are defined as RNA stretches larger than 200 nucleotides, which are not used as a template for translation (Kopp and Mendell 2018; Novikova et al. 2013; Yao et al. 2019). LncRNAs are further divided into mRNA-like intergenic transcripts (lincRNAs), natural antisense transcripts (NATs), MALAT1-associated small cytoplasmic RNA (mascRNAs), SnoRNA-ended lncRNAs (sno-lncRNAs), or covalently closed circular structures (ciRNAs and circRNA) (Kopp and Mendell 2018; St Laurent et al. 2015; Yao et al. 2019).

lncRNAs are implicated in a multitude of processes ranging from embryonic stem cell pluripotency, hematopoiesis, and cell-cycle regulation. They are also involved in numerous diseases such as cancer and cardiovascular pathologies (Alvarez-Dominguez and Lodish 2017; Batista and Chang 2013; Bhan et al. 2017; Chen 2016; Chen et al. 2018; Elling et al. 2016; Fico et al. 2019; Liu et al. 2018; Rinn and Chang 2012; Sallam et al. 2018; Sarropoulos et al. 2019; Schmitz et al. 2016; Uchida and Dimmeler 2015; Yao et al. 2019; Zhang et al. 2017b). Recent studies suggest that exosomal lncRNAs are a novel mediator of cell-to-cell communication, and have essential roles in the tumor microenvironment, metastasis, invasion, chemoresistance (Patel et al. 2017a; Yousefi et al. 2020). LncRNAs are also emerging as biomarkers in various clinical implications, particularly in cancer prognosis (Bhan et al. 2017; Bolha et al. 2017; Carlevaro-Fita et al. 2020; Flynn and Chang 2014; Hu et al. 2012). One of the common themes amongst all these processes is that lncRNAs drive the formation of ribonucleic–protein complexes, which in turn, influence the regulation of gene expression (Rinn and Chang 2012; Zampetaki et al. 2018). This seemingly simple function is performed by three methods: (1) decoys—lncRNA can serve as decoys that prelude the access of regulatory proteins to DNA, (2) scaffold—lncRNAs serve as an adaptor bringing two or more proteins together to performs a specific function, (3) guides—these

lncRNAs are prerequisite for localization of distinct protein complexes (Rinn and Chang 2012). Their primary structure determines these functional properties of RNA. However, RNA is also capable of adopting complex secondary and tertiary structure (Blythe et al. 2016; Johnsson et al. 2014; Kim et al. 2020; Mercer and Mattick 2013; Somarowthu et al. 2015; Zampetaki et al. 2018). Furthermore, such complexity in the structure of lncRNA is higher than that of mRNA, bestowing lncRNA with higher stability, as well as an enhanced capability to bind to proteins and other nucleic acids to undertake gene regulatory functions (Blythe et al. 2016; Clark et al. 2012; Fernandes et al. 2019; Novikova et al. 2013; Wan et al. 2012).

Similar to eukaryotic ncRNAs, other organisms such as bacteria and viruses also contain ncRNAs that play critical roles in their life cycle. For example, Flaviviruses, a group of positive-sense, single-stranded RNA viruses (includes Dengue, Japanese encephalitis, Murray Valley encephalitis (MVEV), Powassan (PowV), West Nile, hepatitis C, and Zika viruses) contain 5′ and 3′ non-coding terminal regions (TR). Several studies have highlighted the critical role of these TRs in viral replication. These terminal regions are intolerable to mutations, often causing lethality or a significant reduction in viral replication (Brinton 2013), and interact with many host proteins required for replication (Ariumi 2014; Brinton 2013; Brinton and Basu 2015; Brinton et al. 1986; Fernández-Sanlés et al. 2017; Li et al. 2013; Tingting et al. 2006). Furthermore, the TRs are also crucial for genome cyclization where the 5′ TR interacts with the 3′ TR to facilitate proper positioning of the viral NS5 RNA-dependent RNA polymerase (Alvarez et al. 2005; Duan et al. 2019; Filomatori et al. 2006; Villordo et al. 2015). In the case of cells infected with Japanese encephalitis virus, it was found that subgenomic flaviviral RNA (sfRNA) acts as a switch that shuts down antigenome synthesis and viral translation, resulting in the packaging and dissemination of mature viral particles from the cells (Fan et al. 2011). Another highlighted role of TRs in family *Flaviviridae* is the 5′ TR IRES (internal ribosomal entry site) of Hepatitis C virus and other genera like *Pegivirus* and *Pestivirus*, which mainly mediates cap-independent translation. The HCV IRES structure and functions have been extensively studied (Lukavsky 2009; Perard et al. 2013; Vopalensky et al. 2018). Critical roles of viral lncRNA are reported in human immunodeficiency virus, herpes simplex virus, and influenza virus. The effects of viral lncRNA include regulation of host immune response, regulation of pathogen proliferation, and maintaining viral latency (Shirahama et al. 2020; Wang et al. 2017).

Despite the variety of roles of ncRNAs, there is a limited understanding regarding their structure(s), primarily due to the length of the molecule(s) enabling multiple conformations to exist at once (Blythe et al. 2016; Gopal et al. 2012; Novikova et al. 2012; Somarowthu et al. 2015). There are two main approaches used to probe the secondary structure of lncRNA, each with its benefits and limitations (Blythe et al. 2016). The first is to predict lncRNA secondary structures using thermodynamic models, which incorporate experimentally determined base-pairing energies. This is a quick method; however, as the length of RNA increases, the determination of secondary structures becomes challenging, as such methods cannot account for long-range interactions. The second approach is to use biochemical techniques such as selective 2′ hydroxyl acylation analyzed by primer extension (SHAPE) (Deigan et al. 2009; Merino et al. 2005), where non-base-pairing nucleotides are chemically modified, and the entire modified RNA is subjected to sequencing. The resultant sequencing readout helps in distinguishing paired nucleotides from unpaired nucleotides. SHAPE allows reliable determination of secondary structure, but it is labor-, time-, and cost-intensive. Readers should refer to (Blythe et al. 2016; Loughrey et al. 2014; Merino et al. 2005; Smola et al. 2015) for details of SHAPE approaches. Furthermore, it is important to mention that unlike sncRNA, it is ultimately the shape and not the sequence which governs the function of lncRNA, as observed in case of protein secondary vs. tertiary structure. Thus, by merely using mutational and sequencing methods, one cannot understand the role of lncRNA (Zampetaki et al. 2018).

To determine the three-dimensional structure of lncRNAs, techniques such as X-ray crystallography, nuclear magnetic resonance, solution X-ray scattering (SAXS), and cryo-electron microscopy can be employed. These techniques are capable of providing a direct representation of the three-dimensional structure of lncRNA. However, a common pitfall for all these techniques is the difficulty in the production of highly purified lncRNAs and maintaining sample integrity. Another challenge is that lncRNAs are susceptible to degradation. Multiple conformations, degraded products, and aggregation can negatively impact data collection and analysis. Therefore, a reliable method is required to characterize the lncRNAs in solution without altering or destroying the samples. AUC offers several advantages over other methods to study the purity and conformations of lncRNAs. For example, the purity, aggregation, oligomerization, and conformational changes of lncRNAs can be studied over a range of concentrations, temperatures, and buffer conditions. AUC requires a minuscule amount of sample as compared to crystallography and other biophysical techniques, and with the advanced sensitive detectors, even minute amounts of aggregation and/or degradation can be accurately detected. This review highlights and discusses the various examples where AUC has been employed to evaluate the purity, homogeneity, binding and hydrodynamic properties of lncRNA in solution.

Non-coding RNA characterization using AUC

Characterization of flaviviral RNAs

As summarized previously, Flaviviral ncRNAs interact with host proteins and are critical for viral life cycle (Meier-Stephenson et al. 2018; Shah et al. 2018). Therefore, it is essential to study their structure and interactions with host proteins. However, as mentioned above, there are many challenges associated with studying ncRNA structures, including the degradation of ncRNAs, multiple conformations, and potential aggregation. Therefore, a thorough quality control analysis of ncRNAs is essential prior to structural studies. AUC has emerged as a reliable tool to evaluate purity, aggregation, and degradation simultaneously.

The first example of the application of AUC is a study by Mrozowich et al. (2020). The authors were interested in studying the structures of MVEV and PowV non-coding TRs using SAXS and computational modeling. Using SAXS, it is possible to derive a low-resolution molecular envelopes of biomolecules (Mrozowich et al. 2018; Patel et al. 2017b). However, since the quality of low-resolution envelops can be affected by the presence of degraded and/or oligomeric species, it was paramount that the quality of RNAs was evaluated accurately. The 5′ and 3′ non-coding TRs were first in vitro transcribed using T7 RNA polymerase, and initial quality assessment steps were performed using urea-PAGE. The urea-PAGE analysis indicated that

the MVEV 5′ TR had minor degradation, whereas the three other RNAs were pure, as judged by a single band. However, denaturing urea-PAGEs are unable to assess the conformational or oligomeric state of RNAs. Therefore, AUC was selected, as it has emerged as a very reliable quality control method.

The AUC-SV data for the size exclusion chromatography (SEC) purified RNAs were collected using a Beckman Optima AUC centrifuge, and an AN50-Ti rotor at 20 °C at 35,000 rpm. Data were processed using the UltraScan-III package (Demeler and Gorbet 2016), which utilized two-dimensional spectrum analysis, van Holde-Weischet, and genetic algorithm analyses. (Brookes et al. 2010; Brookes and Demeler 2007; Demeler and van Holde 2004). The AUC-SV results for all four RNAs are summarized in Fig. 1. The sedimentation coefficient distribution indicates that all four RNAs are mainly monodispersed, with MVEV 5′ TR showing minor degradation, supporting the urea-PAGE analysis. Sedimentation coefficient (*s*) values of 4.27 S and 4.30 S were obtained for MVEV 5′ TR and 3′ TR, respectively (Fig. 1a). The AUV-SV analysis for PowV 5′ and 3′ TRs resulted in *s*-values of 4.49 S and 4.53 S, respectively (Fig. 1b). All four RNAs also displayed peaks at ~ 5.5 S, indicating the presence of oligomeric states in solution. The authors have suggested that this oligomerization could be the result of RNA adopting multiple conformations, which is also suggested by their predicted secondary structures. The AUC-SV analysis also demonstrated that PowV TRs, with a molecular weight (M_w) of ~ 38 kDa, have a marginally higher sedimentation
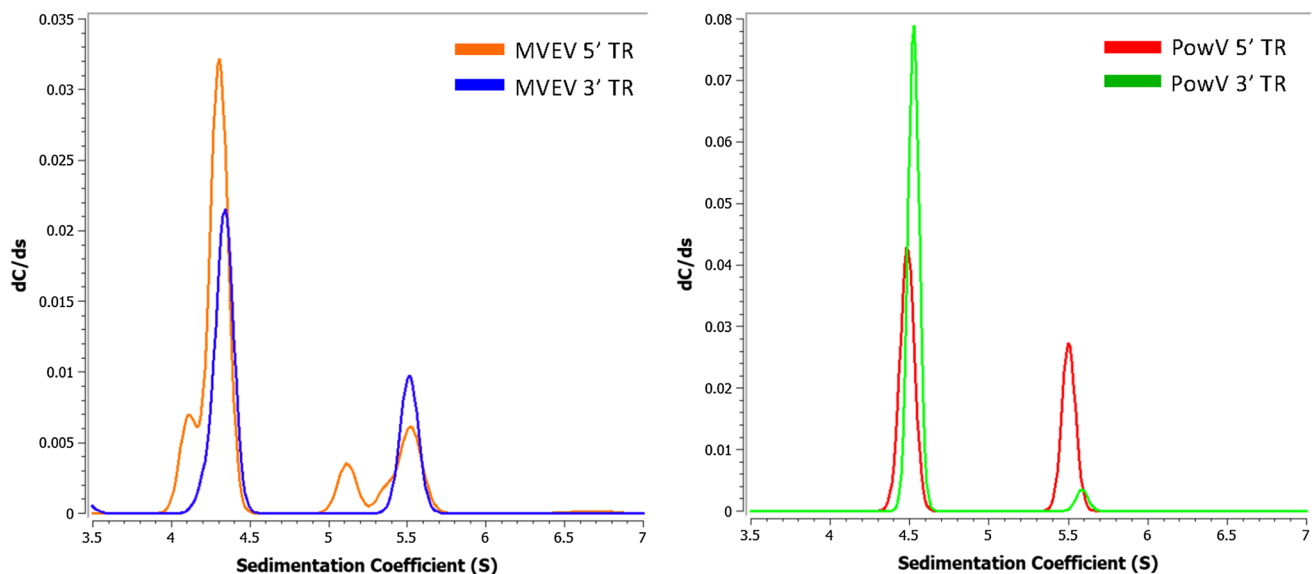
Fig. 1 Solution characterization of in vitro transcribed 5′ and 3′ terminal regions (TRs) of MVEV and PowV RNA. **a** Sedimentation coefficient distribution profiles of MVEV non-coding TRs. **b** Sedimentation coefficient distribution profiles for PowV non-coding TRs. Sedimentation velocity-analytical ultracentrifugation (SV-AUC) The SV peaks at ~ 4.5 S for each RNA represent monomeric fractions. The sedimentation coefficient values are corrected to standard solvent conditions (20 C in water)

coefficient compared to the MVEV TRs with a M_w of ~ 32 kDa. This indicates that these viral TR RNAs have more extended conformations in solution. The detectable difference in s-values of the RNAs with a mere difference of 6 kDa highlights that using sedimentation profiles to characterize RNA is more accurate and can better represent their size and shape. Overall, these experiments suggested that all four RNAs are of suitable purity to perform HPLC-SAXS, but it would be highly inadvisable to perform any SAXS without the use of HPLC to remove minor impurities during data collection.

Another hydrodynamic analysis of a ncRNAs probing a protein–RNA interaction is the recent multi-wavelength AUC (MWL-AUC) study by Zhang et al. (2017a). They studied the hydrodynamics of the 75 nucleotides negative sense 3′ stem-loop RNA of the West Nile virus (WNV) and its affinity with the human T cell-restricted intracellular antigen-1-related protein (hTIAR). In this study, the authors collected MWL-AUC data in the spectral range of 236–294 nm, with 1 nm increment, followed by spectral deconvolution to identify the specific absorption spectra provided by WNV RNA and hTIAR protein components. This approach allowed the assessment of the homogeneity of individual components, as well as the stoichiometric ratios of hTIAR and WNV RNA. The purity of hTIAR and WNV RNA was studied using AUC, followed by an analysis of the mixture of WNV RNA and hTIAR at various ratios (3:1, 6:1, and 10:1 protein: RNA). The MWL-AUC data were analyzed using UltraScan-III (Brookes et al. 2010; Brookes and Demeler 2007). First, two-dimensional spectrum analysis was performed to provide an unbiased hydrodynamic model for each dataset chosen based on the wavelength scans (Brookes et al. 2010). The results were then fitted globally using Monte Carlo analysis to accurately determine the hydrodynamic properties of each analyte (sedimentation and frictional coefficients), as well as the stoichiometry of the reaction (Demeler and Brookes 2008). Overall, this experiment provided a stoichiometry of 4:1 for the hTIAR:WNV RNA interaction. Furthermore, the s-value and anisotropy analysis of a sample containing 10:1 loading ratio of hTIAR:WNV RNA suggested a minor variation in hTIAR anisotropy (1.25–1.75). Moreover, when hTIAR interacted with the WNV RNA, as expected, the s-values increased, with a minute decrease in the anisotropy (1–1.5), suggesting an increased globular conformation of the complex, compared to that of hTIAR alone. The MWL-AUC analysis also suggested a negligible conformational change in WNV RNA upon binding with hTIAR. Overall, this study presented an application of MWL-AUC experiment to investigate stoichiometric ratio, anisotropy, and intermediate species of an RNA–protein complex. Unlike traditional data collection and analysis, application of spectral deconvolution allowed evaluation of these parameters simultaneously.

In summary, the above-mentioned examples of viral RNAs demonstrate that AUC is undoubtedly an essential tool to study ncRNAs homogeneity and interactions.

Characterization of adenovirus virus-associated (VAI) RNA

Viruses employ several mechanisms to recruit host machinery for their entry, gene replication, protein synthesis, and maturation. They also utilize their proteins and nucleic acids to inhibit the hosts' defence system aimed at combating viral infection (Christiaansen et al. 2015; Dzananovic et al. 2018). One such example is the ncRNA of adenovirus, VAI, which interacts with the human innate immune system protein, and the double-stranded RNA-activated protein kinase R (PKR). The innate immune system is our first line of defence mechanisms, although non-specific, provides protection against a wide range of pathogens. The adenovirus employs host RNA polymerase III to synthesize high-amounts of VAI RNA (Reich et al. 1966; Soderlund et al. 1976). VAI is composed of an apical stem-loop region, central stem-loop, terminal stem regions with predominant double-stranded RNA structures, and is ~ 159 nts long. It interacts with the host protein PKR and blocks its dimerization. PKR consists of two double-stranded RNA-binding domains at the N-terminus and a Ser/Thr kinase domain at the C-terminus. In the absence of VAI, the double-stranded binding domains of PKR recognizes viral double-stranded regions, dimerizes, and auto-trans-phosphorylates the kinase domains (Bevilacqua and Cech 1996; Thomis and Samuel 1993). The auto-trans-phosphorylated PKR, in turn, phosphorylates the eukaryotic initiation factor 2, resulting in the inhibition of translation initiation in the host cell (Gale and Katze 1998). However, many viral proteins and RNAs such as VAI target PKR to inhibit its function (Ariyo et al. 2015; Dzananovic et al. 2018).

Many groups, including the Cole and McKenna labs, have worked on understanding the structural features of VAI RNA and its interactions with PKR (Dzananovic et al. 2013, 2014, 2017; Launer-Felty et al. 2015; Mayo and Cole 2017; VanOudenhove et al. 2009; Wong et al. 2011). Their work involved in vitro transcription of VAI RNA and its fragments, purification using SEC, and aggregation/degradation studies using native, as well as denaturing electrophoresis. Most importantly, they used AUC to study the homogeneity of SEC-purified VAI RNA in solution. A representative example shown in Fig. 2 demonstrates that VAI can be in vitro transcribed and purified to homogeneity. The AUC-SV experiment was performed at 0.2 mg/mL using the Beckman Optima XL-I analytical ultracentrifuge (Beckman Instruments, USA) at 20.0 °C (Dzananovic et al. 2014), followed by data processing using the SEDFIT package (Dam and Schuck 2004; Schuck 1998). The AUC-SV experiment
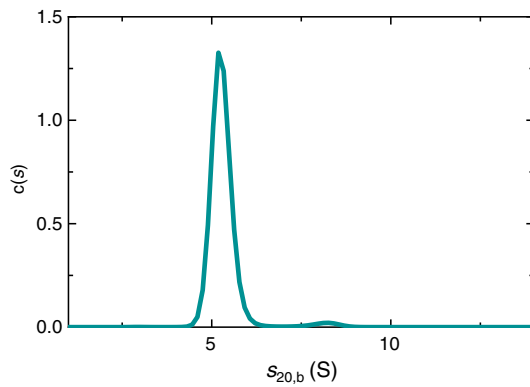
Fig. 2 Sedimentation velocity analysis of adenovirus VAI RNA indicating its purity and sedimentation coefficient of 5.46 S

suggested that the VAI RNA, with a M_w of 48 kDa, has an *s* value of 5.45 ± 0.10 S. Subsequent AUC studies by the Cole group suggested the *s* value of ~ 5.55 S, which agrees with the previous analysis (Launer-Felty et al. 2015). The McKenna group also determined the hydrodynamic radius of VAI RNA (3.80 ± 0.40 nm) (Dzananovic et al. 2014) and combined with the *s* value to determine the molar mass as previously studied (Stetefeld et al. 2016). Their analysis provided a molar mass of 54.2 kDa, which agrees reasonably well with that of a sequence-based molecular weight of 48.2 kDa. Both groups used AUC characterized RNA for SAXS studies to gain insights into the low-resolution structure of full-length VAI RNA. Their SAXS studies suggested that based on Guinier analysis of SAXS data demonstrated that VAI is monodispersed and is devoid of any inter-particle interactions, supporting observations made from AUC-SV experiments (Dzananovic et al. 2014; Launer-Felty et al. 2015). Furthermore, they also demonstrated that VAI RNA adapts an extended and curved shape in solution with a radius of gyration value of ~ 4.4 nm, and the maximum particle dimension of 14–16 nm (Dzananovic et al. 2014; Launer-Felty et al. 2015). In summary, AUC is critical in assessing the purity of ncRNA, prior to performing subsequent experiments for structural and interaction studies.

Characterization of lncRNAs Xist and HOX using AUC

Since lncRNAs are involved in the regulation of various cellular processes such as cell-fate programming, reprogramming, and pluripotency (Carlevaro-Fita et al. 2020; Delas et al. 2019; Leisegang et al. 2017; Sarropoulos et al. 2019), their alteration leads to developmental defects and cancer progression (Flynn and Chang 2014; Hu et al. 2012; Yousefi et al. 2020). LncRNAs are also identified as a biomarker for different stages of osteoarthritis (Zhao and Xu 2018).

AUC has attenuated the challenges and hurdles for the biophysical and structural biology studies of lncRNAs,

which are dynamic and adopt multiple complex conformations (Jones and Sattler 2019; Liu et al. 2018; Somarowthu et al. 2015). In this section, we provide additional examples of another lncRNAs called HOX transcript antisense intergenic RNA (HOTAIR) (Liu et al. 2018; Somarowthu et al. 2015) and mammalian X-inactive specific transcript (Xist) studied using AUC-SV experiments (Liu et al. 2017).

HOTAIR is critical for silencing HoxD genes by interacting with chromatin remodeling enzymes (Rinn et al. 2007; Sparmann and van Lohuizen 2006). The overexpression of lncRNA HOTAIR promotes the metastatic potential of tumors by altering the chromatin dynamics (Gupta et al. 2010). HOTAIR is recognized as a negative prognostic factor in pancreatic cancer (Kim et al. 2013). To investigate the secondary and tertiary structure of HOTAIR, Somarowthu et al. (2015) performed quality assessment using AUC-SV. The authors reported three different purification methods: native, heat cooled, and snap cooled analyzed through AUC-SV. Native purification of HOTAIR showed single homogenous species; however, preparation of samples by heat denaturation and refolding demonstrated inhomogeneous species. (Somarowthu et al. 2015) Next, the authors performed a series of AUC-SV experiments with increasing $MgCl_2$ concentrations and observed an increase in the *s*-value of HOTAIR and a decrease in UV absorption. They demonstrated that an $MgCl_2$ concentration of 25 mM is sufficient to obtain a homogenous preparation of HOTAIR for subsequent structural studies (Somarowthu et al. 2015). Furthermore, the authors also derived the hydrodynamic radius (R_H) of HOTAIR by processing data collected for a series of $MgCl_2$ concentrations using SEDFIT. Subsequently, the R_H derived from the AUC-SV experiment was plotted as a function of Mg^{2+} concentration, to which a Hill equation was fitted. The fit revealed $K_{1/2Mg}$ of 8.6 ± 0.8 mM Mg^{2+} concentration for lncRNA HOTAIR (Somarowthu et al. 2015).

The 5′ TR of Xist is composed of a unique region called RepA. RepA is comprised of 7.5–8.5 copies of a conserved 26-nt motif (made up of A Repeats), which is connected by U-rich linkers. RepA is reported to be involved in transcriptional silencing of the X chromosome (Duszczyk et al. 2011; Wutz et al. 2002). Interestingly, RepA also serves alternative roles as a separate transcript, which is independently transcribed of Xist (Wutz et al. 2002; Zhao et al. 2008). Using AUC-SV, Liu et al. (2017) studied RepA homogeneity and compaction using varying Mg^{2+} concentrations. A series of AUC-SV experiments were performed to monitor the extent of molecular compaction of RepA as a function of Mg^{2+} concentration (Liu et al. 2017), followed by data analysis using SEDFIT (Schuck 2013). It was observed that the *s*-value of RepA gradually increases as a function of Mg^{2+} concentration. These experiments also demonstrate that 15 mM $MgCl_2$ is sufficient to obtain a compact conformation and homogenous preparation of RepA (Liu et al.

2017), suggesting that AUC can be utilized to identify suitable buffer conditions for lncRNA. Incidentally, a study by Romani (2011) indicated that 15–18 mM Mg^{2+} concentration is maintained physiologically in different organelles. Furthermore, the authors also derived R_H of RepA in a series of $MgCl_2$ concentrations using SEDFIT. Similar to their previous studies (Somarowthu et al. 2015), they determined the $K_{1/2Mg}$ to be 4.8 ± 0.2 mM for lncRNA RepA. In summary, AUC provided an optimal concentration range of $MgCl_2$ for RepA folding and homogeneity, which helps to examine the secondary structure profile of RepA using SHAPE and DMS probing and to finally build the computational models based on the experimentally determined secondary structure of RepA.

Thus, AUC studies were instrumental in solving a challenging issue of multiple conformations and misfolding of lncRNAs HOTAIR and Xist as well as other lncRNAs for eventual structural studies.

Concluding remarks

The examples discussed here highlight the importance of applications of AUC in the emerging field of ncRNAs. The capability and adaptability of AUC to characterize biomolecules qualitatively as well as quantitatively makes it a unique technique to ascertain the quality of RNA intended to be used for other experiments. The structural biology techniques employed to determine low- or high-resolution structures of ncRNAs require a pure and monodispersed preparation of ncRNAs and their complexes. AUC offers several benefits over other techniques (e.g., electrophoresis and SEC), such as in-solution measurements, extremely flexible buffer conditions, and a wide range of temperatures. AUC can obtain accurate and reliable information on purity, aggregation, degradation, and detection of multiple conformations of ncRNAs. Therefore, we anticipate that the application of AUC in the ncRNA world will likely increase in the coming years.

References

Alvarez DE, Lodeiro MF, Luduena SJ, Pietrasanta LI, Gamarnik AV (2005) Long-range RNA-RNA interactions circularize the dengue virus genome. J Virol 79:6631–6643

Alvarez-Dominguez JR, Lodish HF (2017) Emerging mechanisms of long noncoding RNA function during normal and malignant hematopoiesis. Blood 130:1965–1975

Arakawa T, Philo JS (1999) Applications of analytical ultracentrifuge to molecular biology and pharmaceutical science. Yakugaku Zasshi 119:597–611

Ariumi Y (2014) Multiple functions of DDX3 RNA helicase in gene regulation, tumorigenesis, and viral infection. Front Genet 5:423

Ariyo EO, Booy EP, Patel TR, Dzananovic E, McRae EK, Meier M, McEleney K, Stetefeld J, McKenna SA (2015) Biophysical characterization of G-quadruplex recognition in the PITX1 mRNA by the specificity domain of the helicase RHAU. PLoS ONE 10:e0144510

Batista PJ, Chang HY (2013) Long noncoding RNAs: cellular address codes in development and disease. Cell 152:1298–1307

Bevilacqua PC, Cech TR (1996) Minor-groove recognition of double-stranded RNA by the double-stranded RNA-binding domain from the RNA-activated protein kinase PKR. Biochemistry 35:9983–9994

Bhan A, Soleimani M, Mandal SS (2017) Long noncoding RNA and cancer: a new paradigm. Cancer Res 77:3965–3981

Blythe AJ, Fox AH, Bond CS (2016) The ins and outs of lncRNA structure: how, why and what comes next? Biochem Biophys Acta 1859:46–58

Bolha L, Ravnik-Glavac M, Glavac D (2017) Long noncoding RNAs as biomarkers in cancer. Dis Mark 2017:7243968

Brautigam CA (2011) Using Lamm-Equation modeling of sedimentation velocity data to determine the kinetic and thermodynamic properties of macromolecular interactions. Methods (San Diego, Calif) 54:4–15

Brautigam CA, Wakeman CA, Winkler WC (2009) Methods for analysis of ligand-induced RNA conformational changes. Methods Mol Biol 540:77–95

Brinton MA (2013) Replication cycle and molecular biology of the West Nile virus. Viruses 6:13–53

Brinton MA, Basu M (2015) Functions of the 3′ and 5′ genome RNA regions of members of the genus Flavivirus. Virus Res 206:108–119

Brinton MA, Fernandez AV, Dispoto JH (1986) The 3′-nucleotides of flavivirus genomic RNA form a conserved secondary structure. Virology 153:113–121

Brookes E, Demeler B (2007) Parsimonious regularization using genetic algorithms applied to the analysis of analytical ultracentrifugation experiments.GECCO '07

Brookes E, Cao W, Demeler B (2010) A two-dimensional spectrum analysis for sedimentation velocity experiments of mixtures with heterogeneity in molecular weight and shape. Eur Biophys J 39:405–414

Carlevaro-Fita J, Lanzos A, Feuerbach L, Hong C, Mas-Ponte D, Pedersen JS, Drivers P, Functional Interpretation G, Johnson R, Consortium P (2020) Cancer LncRNA Census reveals evidence for deep functional conservation of long noncoding RNAs in tumorigenesis. Commun Biol 3:56

Chen LL (2016) Linking long noncoding RNA localization and function. Trends Biochem Sci 41:761–772

Chen X, Sun Y, Cai R, Wang G, Shu X, Pang W (2018) Long noncoding RNA: multiple players in gene expression. BMB Rep 51:280–289

Christiaansen A, Varga SM, Spencer JV (2015) Viral manipulation of the host immune response. Curr Opin Immunol 36:54–60

Clark MB, Johnston RL, Inostroza-Ponta M, Fox AH, Fortini E, Moscato P, Dinger ME, Mattick JS (2012) Genome-wide analysis of long noncoding RNA stability. Genome Res 22:885–898

Cole J, Hansen J (1999) Analytical ultracentrifugation as a contemporary biomolecular research tool. J Biomol Tech 10:163–176

Cole JL, Lary JW, P Moody T, Laue TM (2008) Analytical ultracentrifugation: sedimentation velocity and sedimentation equilibrium. Methods Cell Biol 84:143–179

Crepeau RH, Edelstein SJ, Rehmar MJ (1972) Analytical ultracentrifugation with absorption optics and a scanner-computer system. Anal Biochem 50:213–233

Dam J, Schuck P (2004) Calculating sedimentation coefficient distributions by direct modeling of sedimentation velocity concentration profiles. Method Enzymol 384:185–212

Dean WL, Gray RD, DeLeeuw L, Monsen RC, Chaires JB (2019) Putting a new spin of G-quadruplex structure and binding by analytical ultracentrifugation. Methods Mol Biol 2035:87–103

Deigan KE, Li TW, Mathews DH, Weeks KM (2009) Accurate SHAPE-directed RNA structure determination. Proc Natl Acad Sci USA 106:97–102

Delas MJ, Jackson BT, Kovacevic T, Vangelisti S, Munera Maravilla E, Wild SA, Stork EM, Erard N, Knott SRV, Hannon GJ (2019) lncRNA Spehd regulates hematopoietic stem and progenitor cells and is required for multilineage differentiation. Cell Rep 27(719–729):e716

Demeler B, van Holde KE (2004) Sedimentation velocity analysis of highly heterogeneous systems. Anal Biochem 335:279–288

Demeler B, Brookes E (2008) Monte Carlo analysis of sedimentation experiments. Colloid Polym Sci 286:129–137

Demeler B, Gorbet GE (2016) Analytical ultracentrifugation data analysis with UltraScan-III. In: Uchiyama S, Arisaka F, Stafford WF, Laue T (eds) Analytical ultracentrifugation: instrumentation, software, and applications. Springer Japan, Tokyo, pp 119–143

Duan Y, Zeng M, Jiang B, Zhang W, Wang M, Jia R, Zhu D, Liu M, Zhao X, Yang Q, Wu Y, Zhang S, Liu Y, Zhang L, Yu Y, Pan L, Chen S, Cheng A (2019) Flavivirus RNA-dependent RNA polymerase interacts with genome UTRs and viral proteins to facilitate lavivirus RNA replication. Viruses 11:929

Duszczyk MM, Wutz A, Rybin V, Sattler M (2011) The Xist RNA A-repeat comprises a novel AUCG tetraloop fold and a platform for multimerization. RNA (New York, NY) 17:1973–1982

Dzananovic E, Patel TR, Deo S, McEleney K, Stetefeld J, McKenna SA (2013) Recognition of viral RNA stem-loops by the tandem double-stranded RNA binding domains of PKR. RNA (New York, NY) 19:333–344

Dzananovic E, Patel TR, Chojnowski G, Boniecki MJ, Deo S, McEleney K, Harding SE, Bujnicki JM, McKenna SA (2014) Solution conformation of adenovirus virus associated RNA-I and its interaction with PKR. J Struct Biol 185:48–57

Dzananovic E, Astha CG, Deo S, Booy EP, Padilla-Meier P, McEleney K, Bujnicki JM, Patel TR, McKenna SA (2017) Impact of the structural integrity of the three-way junction of adenovirus VAI RNA on PKR inhibition. PLoS ONE 12:e0186849

Dzananovic E, McKenna SA, Patel TR (2018) Viral proteins targeting host protein kinase R to evade an innate immune response: a mini review. Biotechnol Genet Eng Rev 34:33–59

Elling R, Chan J, Fitzgerald KA (2016) Emerging role of long noncoding RNAs as regulators of innate immune cell development and inflammatory gene expression. Eur J Immunol 46:504–512

Fan YH, Nadar M, Chen CC, Weng CC, Lin YT, Chang RY (2011) Small noncoding RNA modulates Japanese encephalitis virus replication and translation in trans. Virol J 8:492

Fernandes JCR, Acuna SM, Aoki JI, Floeter-Winter LM, Muxel SM (2019) Long non-coding RNAs in the regulation of gene expression: physiology and disease. Noncoding RNA 5:17

Fernández-Sanlés A, Ríos-Marco P, Romero-López C, Berzal-Herranz A (2017) Functional information stored in the conserved structural RNA domains of lavivirus genomes. Front Microbiol 8:546

Fico A, Fiorenzano A, Pascale E, Patriarca EJ, Minchiotti G (2019) Long non-coding RNA in stem cell pluripotency and lineage commitment: functions and evolutionary conservation. Cell Mol Life Sci 76:1459–1471

Filomatori CV, Lodeiro MF, Alvarez DE, Samsa MM, Pietrasanta L, Gamarnik AV (2006) A 5' RNA element promotes dengue virus RNA synthesis on a circular genome. Genes Dev 20:2238–2249

Flynn RA, Chang HY (2014) Long noncoding RNAs in cell-fate programming and reprogramming. Cell Stem Cell 14:752–761

Fujita H (1975) Foundations of ultracentrifugal analysis. Wiley, New York

Gale M Jr, Katze MG (1998) Molecular mechanisms of interferon resistance mediated by viral-directed inhibition of PKR, the interferon-induced protein kinase. Pharmacol Ther 78:29–46

Gillis RB, Rowe AJ, Adams GG, Harding SE (2014) A review of modern approaches to the hydrodynamic characterisation of polydisperse macromolecular systems in biotechnology. Biotechnol Genet Eng Rev 30:142–157

Gopal A, Zhou ZH, Knobler CM, Gelbart WM (2012) Visualizing large RNA molecules in solution. RNA (New York, NY) 18:284–299

Gorbet GE, Mohapatra S, Demeler B (2018) Multi-speed sedimentation velocity implementation in UltraScan-III. Eur Biophys J 47:825–835

Gupta RA, Shah N, Wang KC, Kim J, Horlings HM, Wong DJ, Tsai MC, Hung T, Argani P, Rinn JL, Wang Y, Brzoska P, Kong B, Li R, West RB, van de Vijver MJ, Sukumar S, Chang HY (2010) Long non-coding RNA HOTAIR reprograms chromatin state to promote cancer metastasis. Nature 464:1071–1076

Harding SE (1994) Determination of absolute molecular weights using sedimentation equilibrium analytical ultracentrifugation. In: Jones C, Mulloy B, Thomas A (eds) Methods in molecular biology, vol 22. Humana Press, New Jercy, pp 75–84

Harding SE, Rowe AJ (1988) Automatic data capture and analysis of Rayleigh interference fringe displacements in analytical ultracentrifugation. Opt Lasers Eng 8:83–96

Harding SE, Winzor DJ (2001) Sedimentation velocity analytical ultracentrifugation. In: Harding SE, Chowdhry BZ (eds) Protein–ligand interactions: hydrodynamics and calorimetry. Oxford Univeristy Press, London, pp 75–103

Harding SE, Adams GG, Almutairi F, Alzahrani Q, Erten T, Kok MS, Gillis RB (2015) Ultracentrifuge methods for the analysis of polysaccharides, glycoconjugates, and lignins. Methods Enzymol 562:391–439

Hu W, Alvarez-Dominguez JR, Lodish HF (2012) Regulation of mammalian cell differentiation by long non-coding RNAs. EMBO Rep 13:971–983

Johnson CN, Gorbet GE, Ramsower H, Urquidi J, Brancaleon L, Demeler B (2018) Multi-wavelength analytical ultracentrifugation of human serum albumin complexed with porphyrin. Eur Biophys J 47:789–797

Johnsson P, Lipovich L, Grander D, Morris KV (2014) Evolutionary conservation of long non-coding RNAs; sequence, structure, function. Biochem Biophys Acta 1840:1063–1071

Jones AN, Sattler M (2019) Challenges and perspectives for structural biology of lncRNAs—the example of the Xist lncRNA A-repeats. J Mol Cell Biol 11:845–859

Kim K, Jutooru I, Chadalapaka G, Johnson G, Frank J, Burghardt R, Kim S, Safe S (2013) HOTAIR is a negative prognostic factor and exhibits pro-oncogenic activity in pancreatic cancer. Oncogene 32:1616–1625

Kim DN, Thiel BC, Morozwich T, Hennelly SP, Hofacket IL, Patel TR, Sanbonmatsu KY (2020) Zinc-finger protein CNBP alters the 3-D structure of lncRNA Braveheart in solution. Nat Commun 11:148

Kopp F, Mendell JT (2018) Functional classification and experimental dissection of long noncoding RNAs. Cell 172:393–407

Kung JT, Colognori D, Lee JT (2013) Long noncoding RNAs: past, present, and future. Genetics 193:651–669

Laue TM, Stafford WF III (1999) Modern Applications of analytical ultracentrifugation. Annu Rev Biophys Biomol Struct 28:75–100

Launer-Felty K, Wong CJ, Cole JL (2015) Structural analysis of adenovirus VAI RNA defines the mechanism of inhibition of PKR. Biophys J 108:748–757

Lebowitz J, Lewis MS, Schuck P (2002) Modern analytical ultracentrifugation in protein science: a tutorial review. Protein Sci 11:2067–2079

Leisegang MS, Fork C, Josipovic I, Richter FM, Preussner J, Hu J, Miller MJ, Epah J, Hofmann P, Gunther S, Moll F, Valasarajan C, Heidler J, Ponomareva Y, Freiman TM, Maegdefessel L, Plate KH, Mittelbronn M, Uchida S, Kunne C, Stellos K, Schermuly RT, Weissmann N, Devraj K, Wittig I, Boon RA, Dimmeler S, Pullamsetti SS, Looso M, Miller FJ Jr, Brandes RP (2017) Long noncoding RNA MANTIS facilitates endothelial angiogenic function. Circulation 136:65–79

Li C, Ge LL, Li PP, Wang Y, Sun MX, Huang L, Ishag H, Di DD, Shen ZQ, Fan WX, Mao X (2013) The DEAD-box RNA helicase DDX5 acts as a positive regulator of Japanese encephalitis virus replication by binding to viral 3′ UTR. Antivir Res 100:487–499

Liu J, Yadav S, Andya J, Demeule B, Shire SJ (2015) Analytical ultracentrifugation and its role in development and research of therapeutical proteins. Methods Enzymol 562:441–476

Liu F, Somarowthu S, Pyle AM (2017) Visualizing the secondary and tertiary architectural domains of lncRNA RepA. Nat Chem Biol 13:282–289

Liu M, Zhang H, Li Y, Wang R, Li Y, Zhang H, Ren D, Liu H, Kang C, Chen J (2018) HOTAIR, a long noncoding RNA, is a marker of abnormal cell cycle regulation in lung cancer. Cancer Sci 109:2717–2733

Loughrey D, Watters KE, Settle AH, Lucks JB (2014) SHAPE-Seq 2.0: systematic optimization and extension of high-throughput chemical probing of RNA secondary structure with next generation sequencing. Nucleic Acids Res 42:e165

Lukavsky PJ (2009) Structure and function of HCV IRES domains. Virus Res 139:166–171

MacGregor IK, Anderson AL, Laue TM (2004) Fluorescence detection for the XLI analytical ultracentrifuge. Biophys Chem 108:165–185

Matte SL, Laue TM, Cote RH (2012) Characterization of conformational changes and protein-protein interactions of rod photoreceptor phosphodiesterase (PDE6). J Biol Chem 287:20111–20121

Mattick JS, Makunin IV (2006) Non-coding RNA. Hum Mol Genet 15 Spec No 1:R17–R29

May NA, Wang Q, Balbo A, Konrad SL, Buchli R, Hildebrand WH, Schuck P, Hudson AW (2014) Human herpesvirus 7 U21 tetramerizes to associate with class I major histocompatibility complex molecules. J Virol 88:3298–3308

Mayo CB, Cole JL (2017) Interaction of PKR with single-stranded RNA. Sci Rep 7:3335

Meier-Stephenson V, Mrozowich T, Pham M, Patel TR (2018) DEAD-box helicases: the Yin and Yang roles in viral infections. Biotechnol Genet Eng Rev 34:3–32

Mercer TR, Mattick JS (2013) Structure and function of long noncoding RNAs in epigenetic regulation. Nat Struct Mol Biol 20:300–307

Merino EJ, Wilkinson KA, Coughlan JL, Weeks KM (2005) RNA structure analysis at single nucleotide resolution by selective 2'-hydroxyl acylation and primer extension (SHAPE). J Am Chem Soc 127:4223–4231

Mitra S (2009) Using analytical ultracentrifugation (AUC) to measure global conformational changes accompanying equilibrium tertiary folding of RNA molecules. Methods Enzymol 469:209–236

Mitra S, Demeler B (2020) Probing RNA–protein interactions and RNA compaction by sedimentation velocity analytical ultracentrifugation. Methods Mol Biol 2113:281–317

Mrozowich T, McLennan S, Overduin M, Patel TR (2018) Structural studies of macromolecules in solution using small angle X-ray scattering. J Vis Exp. https://doi.org/10.3791/58538

Mrozowich T, Henrickson A, Demeler B, Patel TR (2020) Nanoscale structure determination of murray valley encephalitis and powassan virus non-coding RNAs. Viruses 12:190

Novikova IV, Hennelly SP, Sanbonmatsu KY (2012) Structural architecture of the human long non-coding RNA, steroid receptor RNA activator. Nucleic Acids Res 40:5034–5051

Novikova IV, Hennelly SP, Tung CS, Sanbonmatsu KY (2013) Rise of the RNA machines: exploring the structure of long non-coding RNAs. J Mol Biol 425:3731–3746

Patel TR, Winzor DJ, Scott DJ (2016) Analytical ultracentrifugation: a versatile tool for the characterisation of macromolecular complexes in solution. Methods (San Diego, Calif) 95:55–61

Patel GK, Khan MA, Bhardwaj A, Srivastava SK, Zubair H, Patton MC, Singh S, Khushman M, Singh AP (2017) Exosomes confer chemoresistance to pancreatic cancer cells by promoting ROS detoxification and miR-155-mediated suppression of key gemcitabine-metabolising enzyme, DCK. Br J Cancer 116:609–619

Patel TR, Chojnowski G, Astha KA, McKenna SA, Bujnicki JM (2017) Structural studies of RNA-protein complexes: a hybrid approach involving hydrodynamics, scattering, and computational methods. Methods (San Diego, Calif) 118–119:146–162

Perard J, Leyrat C, Baudin F, Drouet E, Jamin M (2013) Structure of the full-length HCV IRES in solution. Nat Commun 4:1612

Perkins SJ, Nan R, Li K, Khan S, Abe Y (2011) Analytical ultracentrifugation combined with X-ray and neutron scattering: experiment and modelling. Methods (San Diego, Calif) 54:181–199

Philo JS (1997) An improved function for fitting sedimentation velocity data for low-molecular-weight solutes. Biophys J 72:435–444

Planken KL, Colfen H (2010) Analytical ultracentrifugation of colloids. Nanoscale 2:1849–1869

Reich PR, Forget BG, Weissman SM (1966) RNA of low molecular weight in KB cells infected with adenovirus type 2. J Mol Biol 17:428–439

Rinn JL, Chang HY (2012) Genome regulation by long noncoding RNAs. Annu Rev Biochem 81:145–166

Rinn JL, Kertesz M, Wang JK, Squazzo SL, Xu X, Brugmann SA, Goodnough LH, Helms JA, Farnham PJ, Segal E, Chang HY (2007) Functional demarcation of active and silent chromatin domains in human HOX loci by noncoding RNAs. Cell 129:1311–1323

Romani AM (2011) Cellular magnesium homeostasis. Arch Biochem Biophys 512:1–23

Rowe AJ (2013) Sedimentation equilibrium analytical ultracentrifugation. In: Roberts GCK (ed) Encyclopedia of biophysics. Springer, Berlin, pp 2283–2289

Sallam T, Sandhu J, Tontonoz P (2018) Long noncoding RNA discovery in cardiovascular disease: decoding form to function. Circ Res 122:155–166

Sarropoulos I, Marin R, Cardoso-Moreira M, Kaessmann H (2019) Developmental dynamics of lncRNAs across mammalian organs and species. Nature 571:510–514

Schmitz SU, Grote P, Herrmann BG (2016) Mechanisms of long noncoding RNA function in development and disease. Cell Mol Life Sci 73:2491–2509

Schuck P (1998) Sedimentation analysis of noninteracting and self-associating solutes using numerical solutions to the Lamm equation. Biophys J 75:1503–1512

Schuck P (2013) Analytical ultracentrifugation as a tool for studying protein interactions. Biophys Rev 5:159–171

Schuster TM, Toedt JM (1996) New revolutions in the evolution of analytical ultracentrifugation. Curr Opin Struct Biol 6:650–658

Shah PS, Link N, Jang GM, Sharp PP, Zhu T, Swaney DL, Johnson JR, Von Dollen J, Ramage HR, Satkamp L, Newton B, Huttenhain

R, Petit MJ, Baum T, Everitt A, Laufman O, Tassetto M, Shales M, Stevenson E, Iglesias GN, Shokat L, Tripathi S, Balasubramaniam V, Webb LG, Aguirre S, Willsey AJ, Garcia-Sastre A, Pollard KS, Cherry S, Gamarnik AV, Marazzi I, Taunton J, Fernandez-Sesma A, Bellen HJ, Andino R, Krogan NJ (2018) Comparative flavivirus-host protein interaction mapping reveals mechanisms of dengue and Zika virus pathogenesis. Cell 175(1931–1945):e1918

Sherwood PJ, Stafford WF (2016) SEDANAL: model-dependent and model independent analysis of sedimentation data. In: Uchiyama S, Arisaka F, Stafford WF, Laue TM (eds) Analytical ultracentrifugation instrumentation, software, and applications. Springer Japan, Tokyo, pp 81–102

Shirahama S, Miki A, Kaburaki T, Akimitsu N (2020) Long non-coding RNAs involved in pathogenic infection. Front Genet 11:454

Smola MJ, Rice GM, Busan S, Siegfried NA, Weeks KM (2015) Selective 2′-hydroxyl acylation analyzed by primer extension and mutational profiling (SHAPE-MaP) for direct, versatile and accurate RNA structure analysis. Nat Protoc 10:1643–1669

Soderlund H, Pettersson U, Vennstrom B, Philipson L, Mathews MB (1976) A new species of virus-coded low molecular weight RNA from cells infected with adenovirus type 2. Cell 7:585–593

Somarowthu S, Legiewicz M, Chillon I, Marcia M, Liu F, Pyle AM (2015) HOTAIR forms an intricate and modular secondary structure. Mol Cell 58:353–361

Sparmann A, van Lohuizen M (2006) Polycomb silencers control cell fate, development and cancer. Nat Rev Cancer 6:846–856

St Laurent G, Wahlestedt C, Kapranov P (2015) The landscape of long noncoding RNA classification. Trends Genet 31:239–251

Stetefeld J, McKenna SA, Patel TR (2016) Dynamic light scattering: a practical guide and applications in biomedical sciences. Biophys Rev 8:409–427

Svedberg T, Pedersen KO (1940) The ultracentrifuge. Oxford University Press, Oxford

Thomis DC, Samuel CE (1993) Mechanism of interferon action: evidence for intermolecular autophosphorylation and autoactivation of the interferon-induced, RNA-dependent protein kinase PKR. J Virol 67:7695–7700

Tingting P, Caiyun F, Zhigang Y, Pengyuan Y, Zhenghong Y (2006) Subproteomic analysis of the cellular proteins associated with the 3' untranslated region of the hepatitis C virus genome in human liver cells. Biochem Biophys Res Commun 347:683–691

Uchida S, Dimmeler S (2015) Long noncoding RNAs in cardiovascular diseases. Circ Res 116:737–750

Uchiyama S, Noda M, Krayukhina E (2018) Sedimentation velocity analytical ultracentrifugation for characterization of therapeutic antibodies. Biophys Rev 10:259–269

Unzai S (2018) Analytical ultracentrifugation in structural biology. Biophys Rev 10:229–233

VanOudenhove J, Anderson E, Krueger S, Cole JL (2009) Analysis of PKR structure by small-angle scattering. J Mol Biol 387:910–920

Villordo SM, Filomatori CV, Sanchez-Vargas I, Blair CD, Gamarnik AV (2015) Dengue virus RNA structure specialization facilitates host adaptation. PLoS Pathog 11:e1004604

Vopalensky V, Khawaja A, Roznovsky L, Mrazek J, Masek T, Pospisek M (2018) Characterization of hepatitis C virus IRES Quasi species—from the individual to the pool. Front Microbiol 9:731

Wan Y, Qu K, Ouyang Z, Kertesz M, Li J, Tibshirani R, Makino DL, Nutter RC, Segal E, Chang HY (2012) Genome-wide measurement of RNA folding energies. Mol Cell 48:169–181

Wang Z, Zhao Y, Zhang Y (2017) Viral lncRNA: a regulatory molecule for controlling virus life cycle. Noncoding RNA Res 2:38–44

Wawra SE, Onishchukov G, Maranska M, Eigler S, Walter J, Peukert W (2019) A multi-wavelength emission detector for analytical ultracentrifugation. Nanoscale Adv 1:4422–4432

Wolff M, Unuchek D, Zhang B, Gordeliy V, Willbold D, Nagel-Steger L (2015) Amyloid beta oligomeric species present in the lag phase of amyloid formation. PLoS ONE 10:e0127865

Wong CJ, Launer-Felty K, Cole JL (2011) Analysis of PKR–RNA interactions by sedimentation velocity. Methods Enzymol 488:59–79

Wutz A, Rasmussen TP, Jaenisch R (2002) Chromosomal silencing and localization are mediated by different domains of Xist RNA. Nat Genet 30:167–174

Yang TC, Catalano CE, Maluf NK (2015) Analytical ultracentrifugation as a tool to study nonspecific protein-DNA interactions. Methods Enzymol 562:305–330

Yao RW, Wang Y, Chen LL (2019) Cellular functions of long noncoding RNAs. Nat Cell Biol 21:542–551

Yousefi H, Maheronnaghsh M, Molaei F, Mashouri L, Reza Aref A, Momeny M, Alahari SK (2020) Long noncoding RNAs and exosomal lncRNAs: classification, and mechanisms in breast cancer metastasis and drug resistance. Oncogene 39:953–974

Zampetaki A, Albrecht A, Steinhofel K (2018) Long non-coding RNA structure and function: is there a link? Front Physiol 9:1201

Zhang J, Pearson JZ, Gorbet GE, Colfen H, Germann MW, Brinton MA, Demeler B (2017) Spectral and hydrodynamic analysis of West Nile virus RNA–protein interactions by multi-wavelength sedimentation velocity in the analytical ultracentrifuge. Anal Chem 89:862–870

Zhang X, Hamblin MH, Yin KJ (2017) The long noncoding RNA Malat 1: its physiological and pathophysiological functions. RNA Biol 14:1705–1714

Zhao Y, Xu J (2018) Synovial fluid-derived exosomal lncRNA PCGEM1 as biomarker for the different stages of osteoarthritis. Int Orthop 42:2865–2872

Zhao J, Sun BK, Erwin JA, Song JJ, Lee JT (2008) Polycomb proteins targeted by a short repeat RNA to the mouse X chromosome. Science 322:750–756

Zhao H, Brautigam CA, Ghirlando R, Schuck P (2013) Overview of current methods in sedimentation velocity and sedimentation equilibrium analytical ultracentrifugation. Curr Protoc Protein Sci Chapter 20(Unit20):12